

PAPER • OPEN ACCESS

## On the Problem of the Imperfections of the Structural Glass Members Made of Flat Glass

To cite this article: Ondrej Pesek *et al* 2019 *IOP Conf. Ser.: Mater. Sci. Eng.* **471** 052042

View the [article online](#) for updates and enhancements.

# On the Problem of the Imperfections of the Structural Glass Members Made of Flat Glass

Ondrej Pesek<sup>1</sup>, Jindrich Melcher<sup>1</sup>, Martin Horacek<sup>1</sup>, Ivan Balazs<sup>1</sup>

<sup>1</sup> Institute of Metal and Timber Structures, Faculty of Civil Engineering, Brno University of Technology, Veveří 331/95, 602 00 Brno, Czech Republic

pesek.o@fce.vutbr.cz

**Abstract.** This paper deals with initial geometrical imperfections of the structural glass members made of flat glass. The design of the load bearing glass structures is relatively common in modern architecture, but there is not an Eurocode on design of glass members. Thus, practical design is still a challenge for structural engineers. In the case of structural glass members with problems of lack of stability (columns, beams and beam-columns), it is necessary to know the shape and size of the initial geometrical imperfections to carry out a static design. European product standards of float glass panes distinguish several types of geometrical imperfections. In the frame of this paper, the measurement and evaluation of the most important of them – overall bend – is presented. The initial geometrical imperfections (in the shape of overall bend) were measured on the 33 specimens. But in the real structures we can recognize three types of imperfections: geometrical imperfections of a structural member (imperfect shape), structural imperfections (loading eccentricity, unknown boundary conditions) and physical imperfections (inhomogeneity, residual stresses). These three types of imperfections can be replaced by only one equivalent geometrical imperfection. The only way to find out the size of this imperfection is to carry out an experiment on flexural buckling and lateral torsional buckling. Equivalent geometrical initial imperfections were evaluated using Southwell's plot of flexural buckling and lateral torsional buckling results. The amplitudes of those imperfections were statistically evaluated and with knowing of the 5% quantile of those amplitudes, it is possible to obtain parameters of Eurocode buckling curves.

## 1. Introduction

Structural glass has been established as a material of load carrying members in the end of twentieth century and its importance still grows [1]. Due to slenderness of glass members, it is necessary to check them for stability problems – flexural or lateral torsional buckling or interactions of them. Design methods of steel and timber structures are not completely usable for glass structures because of several differences (initial imperfections, brittle behaviour and laminated glass behaviour) [2]. The shape and size of initial geometrical imperfections are poorly published in recent publications.

Behaviour of imperfect columns and beams under loading was published in [3]. Equation (1) [3, 4] describes (according to the second order theory) dependency of deformation  $f(w_0)_x$  of axially loaded imperfect column and bended beams (Figure 1a) on amplitude of initial imperfection. Sinusoidal shape of overall bow (see Figure 2) imperfection is considered. Flexural deformation increases with increasing amplitude of initial imperfection (see Figure 1b).



$$f(w_0)_x = w_0 \frac{N}{N_{cr} - N} \cdot \cos \frac{\pi \cdot x}{L} \quad v(x) = \frac{c_1 \cdot \frac{G \cdot I_t}{E \cdot I_z} \cdot M_y \cdot \varphi_0 + c_1^2 \cdot \frac{M_y^2}{E \cdot I_z} \cdot v_0}{G \cdot I_t \cdot \left(\frac{\pi}{L}\right)^2 - \frac{c_1^2 \cdot M_y^2}{E \cdot I_z} + c_2 \cdot \left(\frac{\pi}{L}\right)^2 \cdot M_y \cdot z_g} \cdot \cos\left(\frac{\pi}{L} \cdot x\right) \quad (1)$$

where:

$w_0; \varphi_0; v_0$  — is amplitude of initial imperfections [mm, rad],  
 $N; M_y$  — axial force, bending moment [N, Nmm],  
 $N_{cr}$  — Euler's critical force [N],  
 $L$  — buckling length [mm],  
 $E; G$  — Young's modulus, shear modulus [MPa],  
 $I_t; I_z$  — cross sectional characteristics [mm<sup>4</sup>],  
 $x$  — point of interest, distance from mid-span [mm].

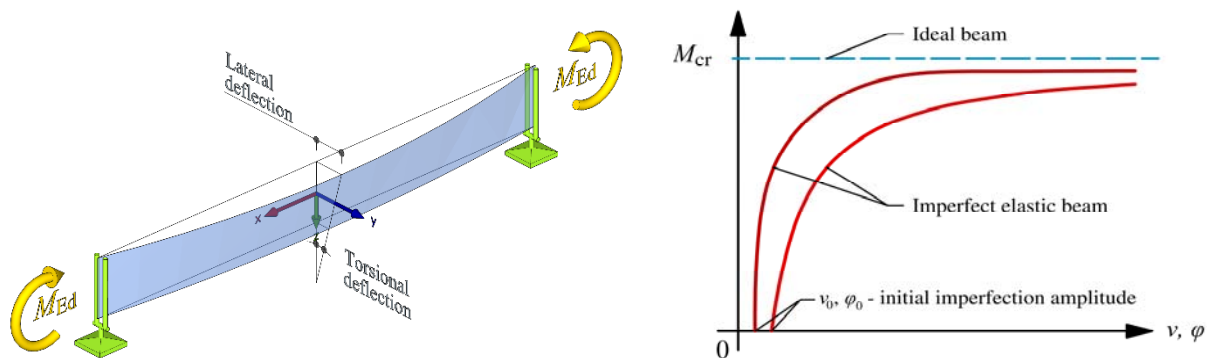


Figure 1. a) Lateral-torsional buckling model, b) Bending moment-deflection relationship

## 2. Initial geometrical imperfections

The differences of nominal dimensions are generated during manufacturing processes and they should be lower than limits specified in product standards. Following tolerances should be checked: (i) glass pane thickness, (ii) glass pane length, wide and rectangularity, (iii) edge deformations due to vertical production (does not apply on float glass) and (iv) planarity (flatness).

Geometrical deformations (curvature) result from glass tempering processes (manufacturing process of fully tempered glass or heat strengthened glass). The size of deformations depends on type of glass (coated glass, patterned glass etc.), on glass dimensions and aspect ratio, on nominal thickness and on type of tempering process (vertical or horizontal).

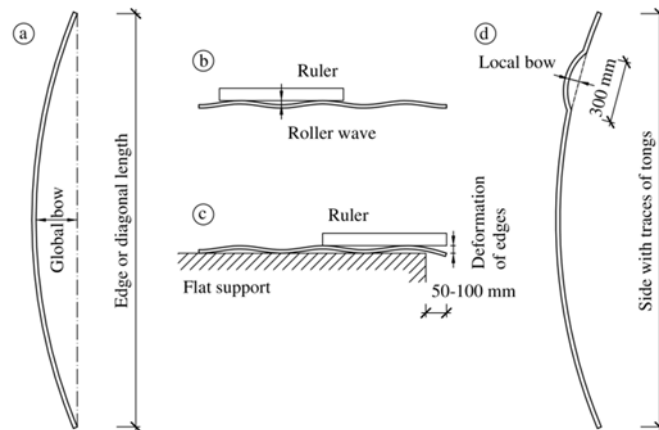


Figure 2. Glass pane deformations types

There are four types of deformations: (a) overall bow, (b) roller wave (only for horizontally tempered glass), (c) curvature of edges (only for horizontally tempered glass) and (d) local bow (only for horizontally tempered glass) – see Figure 2.

The maximum allowable values of the overall bow deflection according to the EN 1863-1 [5] and EN 12150-1 [6] are: (i) 3.0 mm/m for float glass horizontally tempered, (ii) 4.0 mm/m for horizontally tempered glass (other types) and (iii) 5.0 mm/m for vertically tempered glass (all types) = see table 1.

**Table 1.** List of maximum allowed imperfections according to the EN 1863-1 [5] and EN 12150-1 [6]

Glass type	Position at tempering	FTG or HSG glass	
		Global bow [mm/m]	Local bow [mm/300 mm]
Float glass without coating	Horizontal	3.0	0.3
Others	Horizontal	4.0	0.5
All	Vertical	5.0	1.0

## 2.1. Methods

Measured specimen was fixed in a vertical position (due to dead load deflections elimination) and supported by two timber blocks according to EN 1863-1 and EN 12150-1. Permanent stability of glass was ensured by a steel stand.

**2.1.1. Specimens.** Initial geometrical imperfections (global bow) were measured on specimens listed in table 2.

**Table 2.** List of specimens

Type of glass	Description	Dimensions [mm]			Measuring device	Pcs.
		Length	Width	Thickness		
ESG 12	Safety glass	1500	150	12	Carl Zeiss	3
VG 66.2	Laminated glass with PVB foil	1500	150	6+6	Carl Zeiss	3
VSG 66.2	Laminated safety glass with EVASAFE foil	1500	150	6+6	Carl Zeiss	6
VSG 444.33	Laminated safety glass with EVASAFE foil	1500	150	4+4+4	Carl Zeiss	3
VG 1010.2	Laminated glass with EVA foil	2400	280	10+10	own	3
VG 88.2	Laminated glass with PVB foil	2400	280	8+8	own	3
VG 66.2	Laminated glass with PVB foil	2400	280	6+6	own	3
VSG 88.2	Laminated safety glass with EVASAFE foil	2000	200	8+8	own	3
VG 88.2	Laminated glass with PVB foil	2000	200	8+8	own	6
<b>Sum</b>						<b>33</b>

**2.1.2. Measuring set-up.** Overall bow shape of glass specimens was analysed using three devices (Figure 3): laser scan (FARO Focus3D 120); mechanical measuring system Carl Zeiss (with mechanical sensor Carl Zeiss 003 19) and measuring device of own construction (with use of digital gauge Mitutoyo Absolute Digimatic ID-C with accuracy 0.01 mm used).

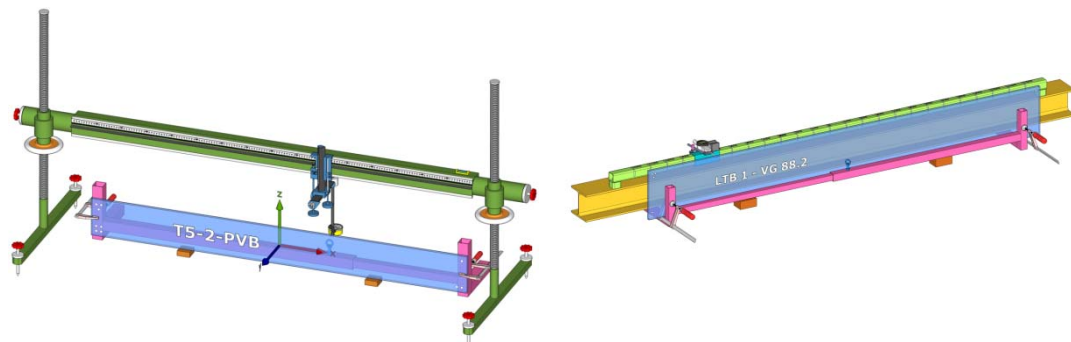


**Figure 3.** Measurement set-up with a) Carl-Zeiss equipment and b) Own construction equipment

**2.1.3. Measuring set-up imperfections.** Because of elimination of measurement errors due to geometrical imperfections of the measuring set up, every specimen and both its edges were measured in two locations - positive location and negative (mirrored) location. The geometrical imperfection of the guiding rail was deducted from measuring the initial shape imperfections of the same glass specimen twice: once in the conventional location and once in the mirrored location. Compensating method [7] is described in Figure 4.

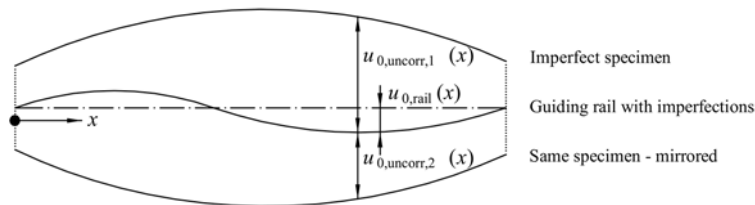


**Figure 4.** Determination of guiding rail imperfections

Using this principle, the shape of imperfection of the guiding rail  $u_{0,rail}(x)$  was determined with (2). Repeating this process several times, the imperfections of the guiding rail could be reproduced with high accuracy. The resulting corrected geometrical imperfection  $u_0(x)$  was obtained using (3).

$$u_{0,rail}(x) = \frac{u_{0,uncorr,1}(x) - u_{0,uncorr,2}(x)}{2} \quad (2)$$

$$u_0(x) = u_{0,uncorr}(x) \pm u_{0,rail}(x) \quad (3)$$

Shapes of imperfections of the guiding rail are plotted in Figure 5 for both measuring devices. To evaluate initial imperfections of all specimens, the mean value of guiding rail imperfections was taken into account. The shape of initial imperfections from all measurements is similar, but on the other hand, the amplitudes are relatively different.

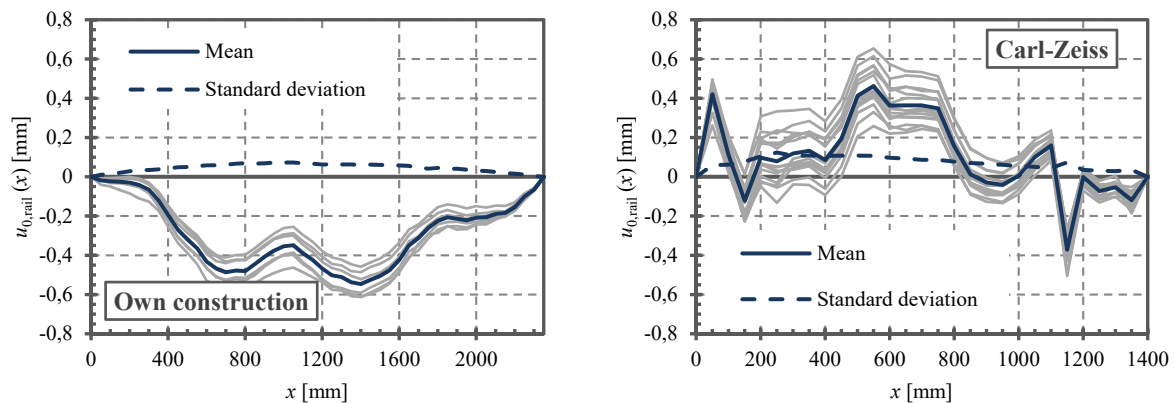


**Figure 5.** Measured shapes of measurement devices

## 2.2. Results

**2.2.1. Size and shape of initial imperfections.** Evaluation of the measurement was carried out according to the approach presented by Belis et al. [7]. Imperfections of all specimens are evaluated with positive sign. The value of initial imperfection  $u_0/L$  represents maximum relative amplitude, which is not generally situated in the half of length of specimen. Relative imperfection amplitudes are plotted in Figure 6a according to the glass type. Mean value is 0.42 mm/m and maximum value is 1.6 mm/m that is much lower than allowable values (Table 1).

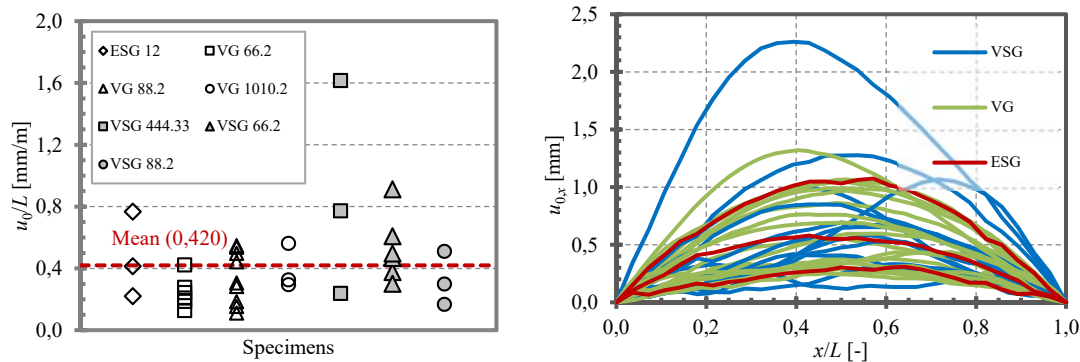


**Figure 6.** a) Relative amplitudes of initial imperfections of tested specimens; b) Imperfect shapes of glass rods

Graph in Figure 6b shows actual shapes of glass member measurements. Curves are coloured according to the glass type. On horizontal axis, length of specimens is plotted in relative units. The shape of initial imperfections could be substituted by a sinusoid or a parabola. Preference is given to the sinusoidal function because it is corresponding to the eigen-mode, which is often adopted as initial geometrical imperfection in buckling analysis [8].

**2.2.2. Statistical evaluation.** For practice design it is necessary to know the characteristic value of initial imperfection  $(u_0/L)k$ , which is entering into linear buckling analysis. Generally, characteristic value is considered as 5% quantile (4). The results of initial imperfection measurements were evaluated such that all imperfection values were positive. Actually, the curvature might be convex or concave and mean value of large population is theoretically equal to zero agreement with the Probabilistic Model Code [9] by JCSS (The Joint Committee on Structural Safety). Histogram of truncated data set with normal distribution function is illustrated in Figure 7a.

$$5\% \text{ quantile} = \mu + 1.645 \cdot \sigma \quad (4)$$

An alternative approach is to directly analyse the asymmetric probability density function based on original 33 imperfection measurement values only. Histogram of original data set with lognormal distribution function is illustrated in Figure 7b. Characteristic value (5% quantile) was calculated by STATISTICA software [10].

Characteristic values of initial imperfections were calculated for annealed glass, fully tempered glass and for both types together using both methods (normal and lognormal distribution). 5% quantile is 1.004 mm/m and 0.936 mm/m for normal and lognormal distribution respectively. The similar values (difference 7 %) show correctness of both methods.

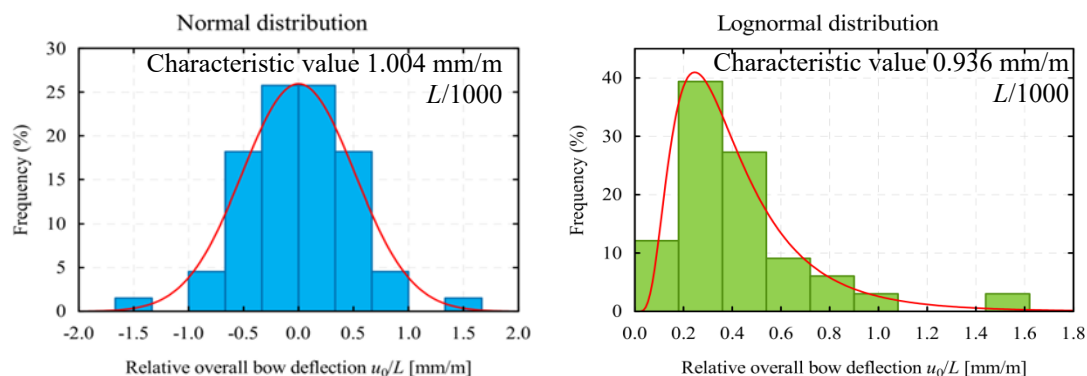


**Figure 7.** Histograms of relative overall bow deflections: a) normal distribution; b) lognormal distribution

### 3. Equivalent geometrical imperfections

In the real structures, we can recognize three types of imperfections: geometrical imperfections of structural member (imperfect shape of member = overall bow and local imperfections), structural imperfections (loading eccentricity, unknown boundary conditions) and physical imperfections (material inhomogeneity, residual stresses). These three types of imperfections can be replaced by only one equivalent geometrical imperfection. The only way to find out the size of the equivalent geometrical imperfection is to carry out an experiment and evaluate the results by Southwell's plot.

#### 3.1. Flexural buckling

In the frame of the experimental analysis, 15 specimens were tested (2). All specimens had the same geometry but a different composition: specimens were made of one, two or three panes of float glass or fully tempered glasses that were bonded together by PVB foil or EVASAFE foil. Overall glass thicknesses were 12 (12, 6+6 or 4+4+4) millimetres in all cases. The test set-up of flexural buckling experimental analysis is plotted in Figure 8a. Behaviour of glass columns is described by  $P$ - $\Delta$  curves in Figure 8b.

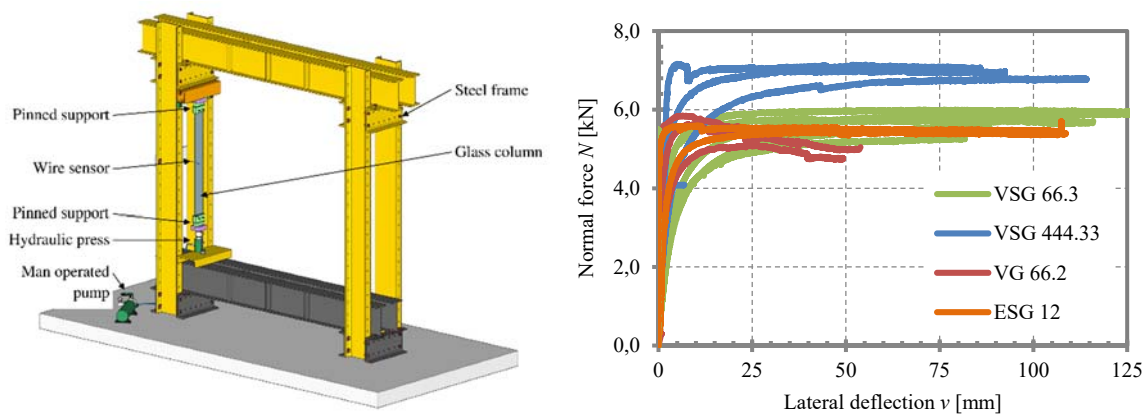


Figure 8. Flexural buckling. (a) Test set-up, (b)  $P$ - $\Delta$  curves

#### 3.2. Lateral-torsional buckling

In the frame of the experimental analysis, nine specimens were tested (11). All specimens had the same geometry (length 2400 mm, depth 280 mm) but a different composition: specimen was made of two glass panes of float glass that were bonded together by PVB foil. Overall glass thicknesses were 12 (6+6), 16 (8+8) or 20 (10+10) millimetres. The test set-up of lateral torsional buckling experimental analysis is plotted in Figure 9a. Behaviour of glass beams is described by  $P$ - $\Delta$  curves in Figure 9b.

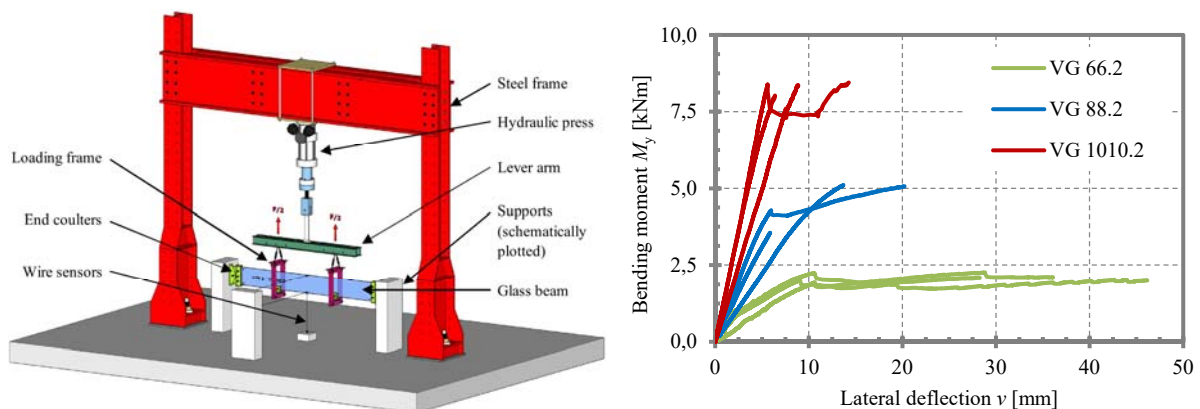
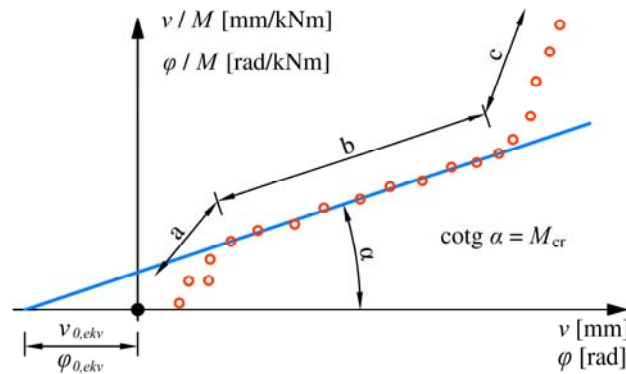


Figure 9. Lateral-torsional buckling. (a) Test set-up, (b)  $P$ - $\Delta$  curves



### 3.3. Southwell's plot

The principle of Southwell's plot is plotted in Figure 10 [3]. This method was applied on results of flexural buckling and lateral-torsional buckling to obtain initial lateral imperfections and initial lateral and torsional imperfections, respectively.



**Figure 10.** Southwell's plot

Amplitudes of equivalent geometrical imperfections were statistically evaluated. 5% quantile of flexural buckling imperfections are 2.148 mm/m and 2.913 mm/m for normal and lognormal statistical distribution respectively – see Figure 11.

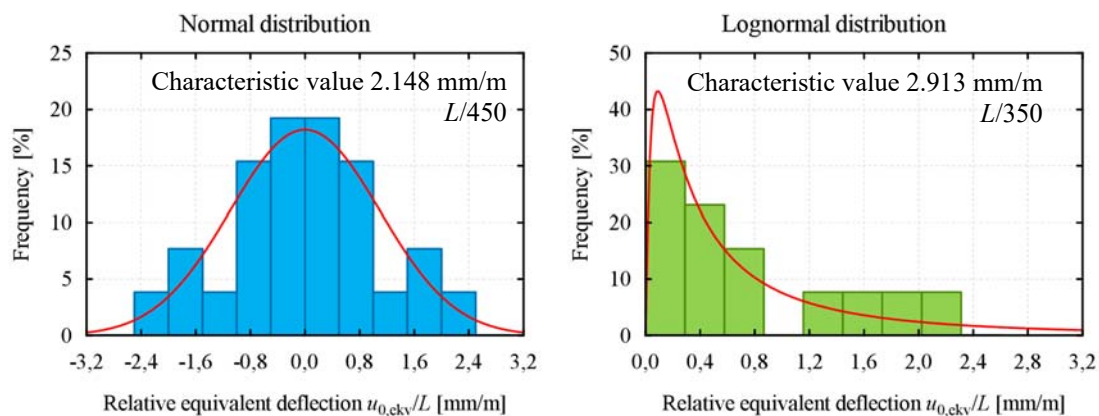


**Figure 11.** Flexural buckling: Normal and lognormal statistical distribution of equivalent initial imperfections

5% quantile of lateral torsional buckling imperfections are 5.129 mm/m and 4.542 mm/m for normal and lognormal statistical distribution respectively – see Figure 12.

## 4. Results

Characteristic value (5% quantile) of geometrical imperfection (for all types of glass together) was  $(u_0/L)_k \approx 1.00$  mm/m (calculated value corresponds to the relative imperfections  $L/1000$ ). For annealed glass ANG  $(u_0/L)_k = 0.652$  mm/m and for fully tempered glass FTG  $(u_0/L)_k = 1.230$  mm/m. It means that limits in standards are not exceeded (limit value for fully tempered glass is 3.00 mm/m for horizontal tempering, for annealed glass the limit value is not defined) – see Figure 13.



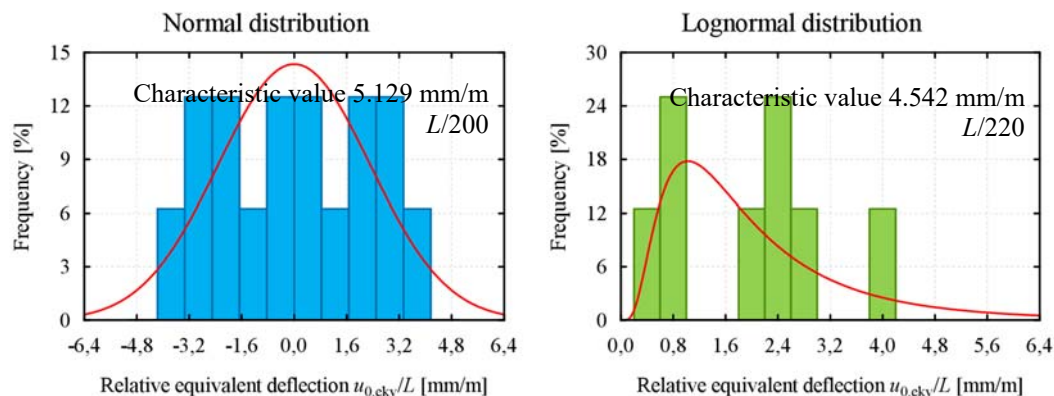


**Figure 12.** Lateral-torsional buckling: Normal and lognormal statistical distr. of equivalent initial imperfections

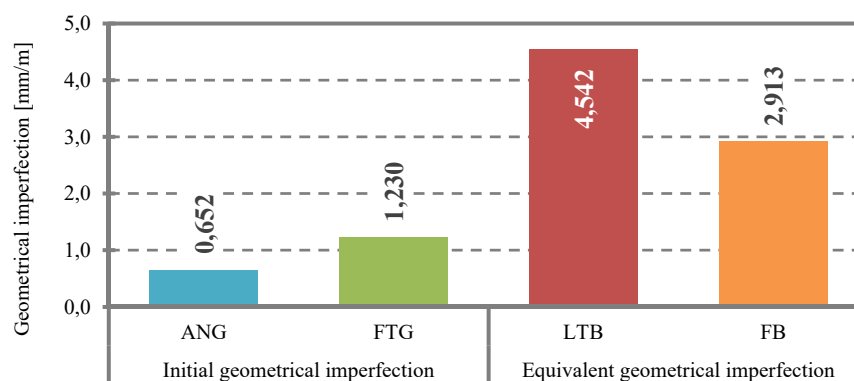


**Figure 13.** 5% quantiles of geometrical imperfections: influence of glass type and stability problem

Using Southwell's plot, the equivalent initial imperfections were found out and they were statistically evaluated for flexural buckling FB and lateral torsional buckling LTB separately. 5% quantile of equivalent imperfections is 4.542 mm/m and 2.913 mm/m, respectively (these values correspond to the relative imperfections  $L/200$  and  $L/350$ ) – see Figure 13.

## 5. Conclusions

This paper summarizes results of measuring of geometrical imperfections of laminated glass members. The shape of imperfections was detected as sinusoidal (in approximation) and size was statistically evaluated. Equivalent geometrical imperfections were calculated using Southwell's plot and these values were statistically evaluated.

## Acknowledgment

The paper was elaborated within the frame of the research program of the Faculty of Civil Engineering, Brno University of Technology No FAST-S-18-5550 and within the project No LO1408 AdMaS UP – Advanced Materials, Structures and Technologies, supported by the National Sustainability Program I of the Ministry of Education, Youth and Sports of the Czech Republic.

## References

- [1] M. Haldimann, A. Luible, M. Overend, "Structural Use of Glass," Zurich: ETH Zurich, 2008. ISBN 3-85748-119-2.

- [2] O. Pešek, J. Melcher, M. Horáček, "Experimental Verification of the Buckling Strength of Structural Glass Columns. In *Procedia Engineering*, Volume 161, 2016, pp. 556-562, ISSN 1877-7058, doi:10.1016/j.proeng.20106.08.691.
- [3] V. Březina, "Buckling Load Capacity of Metal Rods and Beams," (Vzpěrná únosnost kovových prutů a nosníků). Prague: Czechoslovak Academy of Science, 1962.
- [4] R. Kasper, "Tragverhalten von Glasträgern," Aachen, 2005. Ph.D. thesis. RWTH Aachen
- [5] *EN 1863-1. Glass in building – Heat strengthened soda lime silicate glass – Part 1: Definition and description*. European Committee for Standardization, Brussel. ref. number EN 1863-1:2011 E.
- [6] *EN 12150-1. Glass in building – Thermally toughened soda lime silicate glass – Part 1: Definition and description*. European Committee for Standardization, Brussel. ref. number EN 12150-1:2000 E.
- [7] J. Belis, D. Mocibob, A. Luible, M. Vandebroek, "On the size and shape of initial out-of-plane curvatures in structural glass components. *Elsevier Ltd., Construction and Building Materials*. 2011, vol. 25, Issue 5, pp. 2700-2712. ISSN: 0950-0618.
- [8] O. Pešek, J. Melcher, "Measuring and Evaluation of the Shape and Size of Initial Geometrical Imperfections of Structural Glass Members," In *WSEAS Transactions on Applied and Theoretical Mechanics*, Volume 10, 2015, pp. 253-259, ISSN 1991-8747, E-ISSN: 2224-3429
- [9] *JCSS probabilistic model code*. The joint committee on structural safety [online]. 2001 [cit. 2014-12-15]. Available from: <https://www.jcss.byg.dtu.dk>.
- [10] *StatSoft Inc. STATISTICA © Cz 12*, [software]. Available from: <https://www.statsoft.com>.
- [11] O. Pešek, J. Melcher, "Lateral-Torsional Buckling of Laminated Structural Glass Beams. Experimental Study," In *Procedia Engineering*, Volume 190, 2017, pp. 70-77, ISSN 1877-7058, doi:10.1016/j.proeng.2017.05.309.